<h1 style="text-align:center">Supplementary Information</h1>

Designing oxygen bonding reduced graphene oxide encapsulate multishelled Mn₃O₄ hollow spheres for enhanced performance of supercapacitors

Henan Jia†, Zhaoyue Wang†, Chun Li, Xiaoqing Si, Xiaohang Zheng*, Yifei Cai, Jinghuang Lin, Haoyan Liang, Junlei Qi*, Jian Cao, Jicai Feng, Weidong Fei*

State Key Laboratory of Advanced Welding and Joining, Harbin Institute of Technology, Harbin 150001, China

*Corresponding authors: Tel. /fax: 86-451-86418146;

†These authors contributed equally.

E-mail: jlqi@hit.edu.cn (J L Qi)

Experimental Section

Synthesis of Mn-CPs. All the chemicals were directly used after purchase without further purification. In a typical synthesis, 1 mmol of $Mn(NO_3)_2 \cdot 4H_2O$ and 1 mmol of isophthalic acid (H_2IPA) were added to a mixture of 50 mL DMF and 50 mL acetone under stirring to obtain a homogeneous apparent solution. After 6 h stirring, the result clear solution was transferred into a sealed Teflon-lined stainless-steel autoclave and maintained at 160 °C for 4 h. After cooling down to room temperature, the assynthesized precursors were separated by centrifugation and dried at 70 °C for 6 h.

Synthesis of multishelled Mn₃O₄ hollow sphere. The as synthesized Mn-CPs were annealing at 300 °C in air for 10 min with different heating rate ranging from 1 to 10 °C min⁻¹. And the shell numbers can be controlled from 1 to 4 with different heating

rate.

Synthesis of Mn$_3$O$_4$-rGO-x (x=1,2,3). Graphene oxide (GO) was synthesized from natural flake graphite powder via chemical exfoliation (modified Hummers' method), as reported previously. Mn$_3$O$_4$-rGO-x was fabricated by coating GO nanosheets on hydroxyl modified multishelled Mn$_3$O$_4$ hollow spheres, follow by reduction of GO via thermal treatment. The hydroxyl modified process was described as follow. Typically, 0.1 g of the multishelled Mn$_3$O$_4$ hollow spheres were dispersed in 100 ml DI water containing 10 ml ammonium hydroxide, followed by stirring overnight to obtain hydroxyl modified multishelled Mn$_3$O$_4$ hollow spheres. After washing, the product was dispersed in 100 ml distilled water and then mixed with 50 ml aqueous GO suspension with different GO weight. After stirring for 2 h, the product was collected via centrifugation, and then treated at 400 ^{o}C for 2 h in Ar atmosphere in order to achieve the reduction of GO. The samples were labelled as Mn$_3$O$_4$-rGO-x, x=1, 2 and 3 mean the weight of GO are 50 mg, 100 mg and 200 mg, respectively.

Synthesis of oxygen vacancies less Mn$_3$O$_4$: The as synthesized Mn-CPs were annealing at pure O$_2$ and the other parameters remain the same to obtain oxygen vacancies less Mn$_3$O$_4$.

Synthesis of Mn$_3$O$_4$/rGO: All parameters remain unchanged except oxygen vacancies less Mn$_3$O$_4$ as precursor. And the weight of GO is 100mg.

Materials characterization: The morphology and structure of the samples were characterized by SEM (Helios Nanolab 600i) and TEM (Tecnai G2 F30), respectively. XRD was performed using a D/max 2550 with graphite monochromatized Cu Kα radiation.

Electrochemical Performance Measurements: Electrochemical measurements were conducted in a typical three-electrode cell. The samples were used as working

electrodes. Pt foil as the counter electrodes and a saturated calomel electrode (SCE) as reference electrodes in 2 M KOH electrolyte. The working electrodes were prepared by mixing 70 wt% of active material, 20 wt% of carbon black, and 10 wt% of polyvinylidene fluoride (PVDF) in an N-methyl-2-pyrrolidone (NMP) solution to make a slurry. Then, it was coated onto the Ni foam substrate and dried in a vacuum oven at 60 $^\circ$C for 12 h. The mass loading of active materials is ~2.1 mg cm^2. CV curves and the galvanostatic cycling test of the electrodes were carried out on a CHI 760D electrochemical workstation. Electrochemical impedance spectroscopy (EIS) measurements were performed on PARSTAT 4000A electrochemical workstation, over a frequency range from 10^5 to 10^{-1} Hz, at an amplitude of 5 mV.

Fabrication of the asymmetric supercapacitor: The Mn$_3$O$_4$-rGO-2 was used as the positive electrode and the commercial active carbon served as the negative electrode. To fabricate the ASC, the charge balance theory (q$^+$=q$^-$) between positive and negative electrodes should be complied with and the mass ratio between the positive materials and the negative materials were calculated according to the following equation:

$$\frac{m^-}{m^+} = \frac{C^+ \times \Delta V^+}{C^- \times \Delta V^-}$$

where m is the mass of the electrode materials, C is the specific capacitance, ΔV is the range of the potential applied in the charge/discharge process and the "+", "-" are the symbols of positive, negative materials, respectively. Based on the specific capacitance of the electrodes calculated in the three-electrode system and the equation above, the mass of AC is 1.84 times that of the positive electrodes. So the proper mass loading of the ASC is 2.1 mg of Mn$_3$O$_4$-rGO-2 and 3.9 mg of AC.
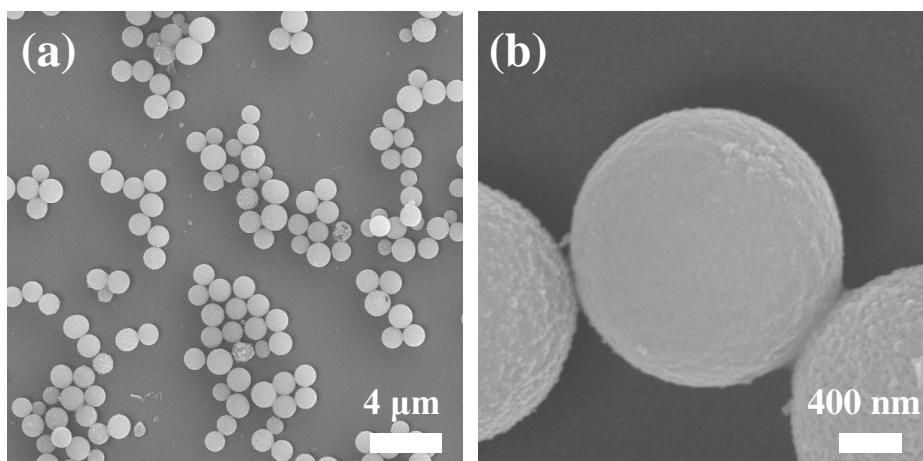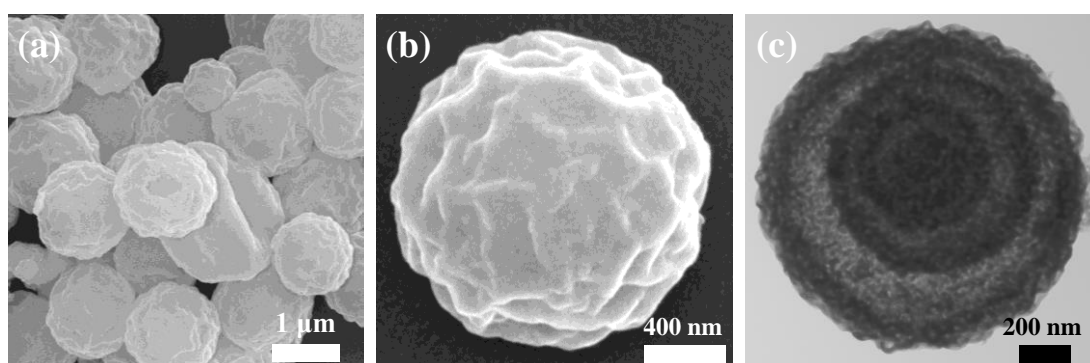
Figure S1. SEM images of Mn-CPs.

Figure S2. a) and b) SEM images, c) TEM image of the Mn-CPs after thermal treatment at heating rate of 0.5 °C min^{-1}.
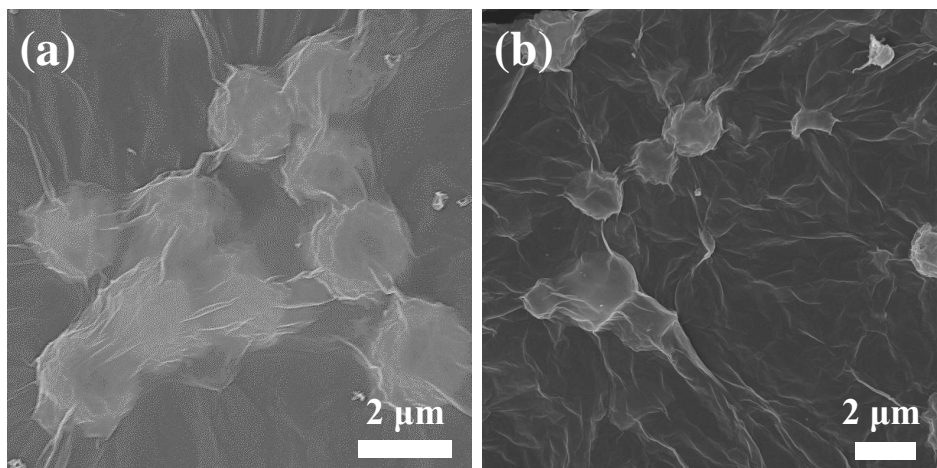
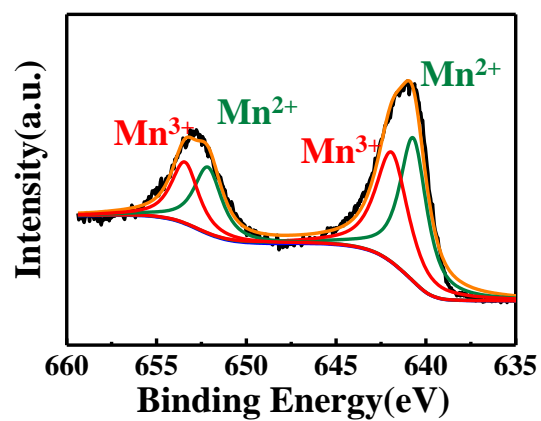**Figure S3.** SEM images of a) Mn_3O_4-rGO-1, b) Mn_3O_4-rGO-3.

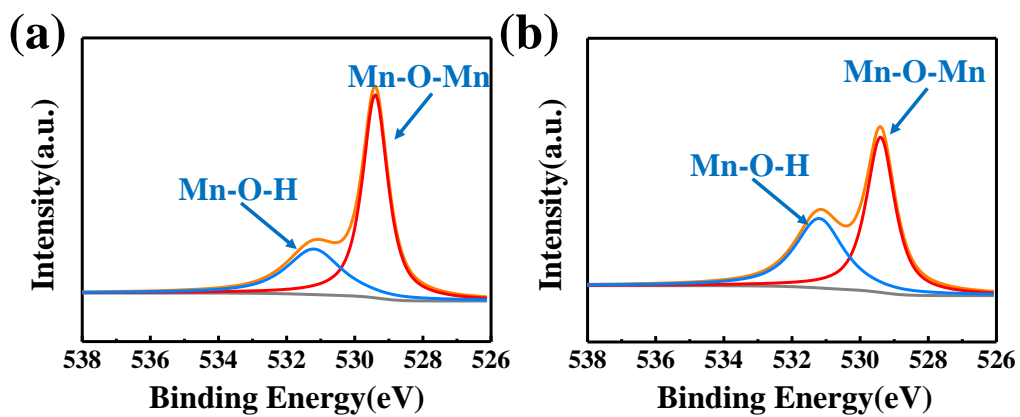**Figure S4.** XPS spectrum of Mn 2p of multishelled Mn_3O_4 hollow spheres.

Figure S5. O 1s spectrum of a) multishelled Mn_3O_4 hollow spheres, b) OH group modified multishelled Mn_3O_4 hollow spheres.
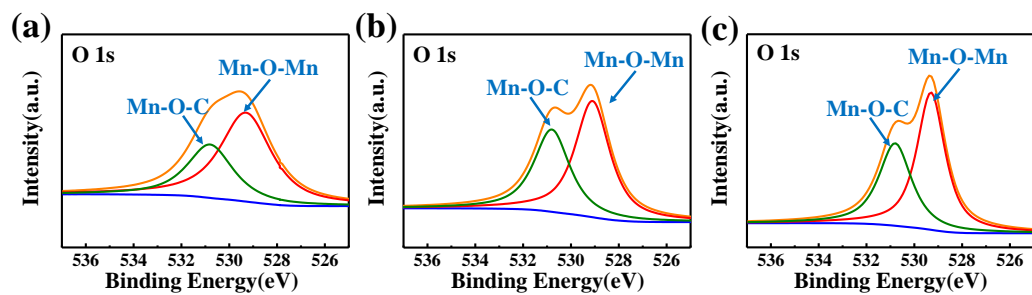

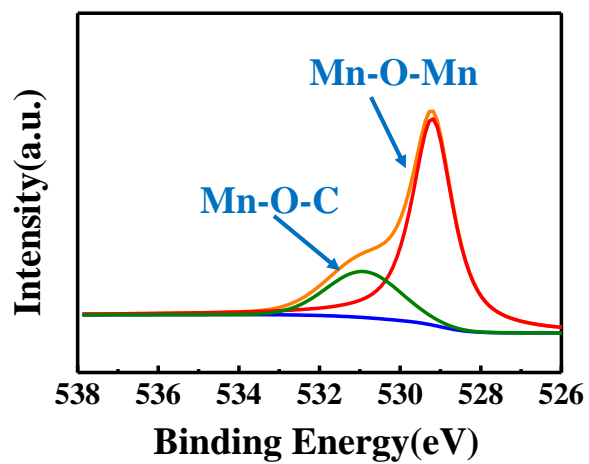**Figure S6.** The O 1s core-level spectra of a) Mn_3O_4-rGO-1, b) Mn_3O_4-rGO-2 and c) Mn_3O_4-rGO-3.
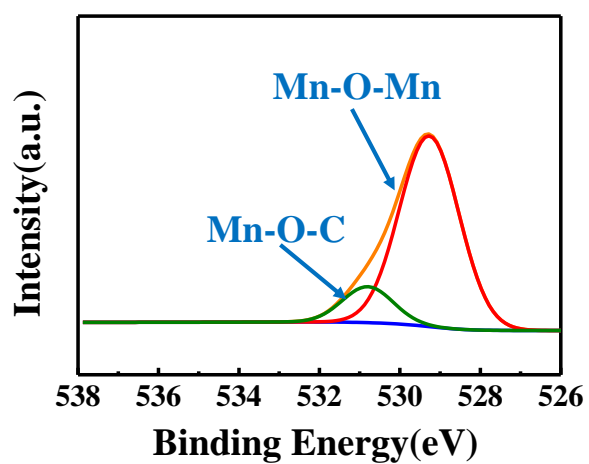
Figure S7. O 1s spectrum of oxygen vacancies less Mn_3O_4-rGO-2.

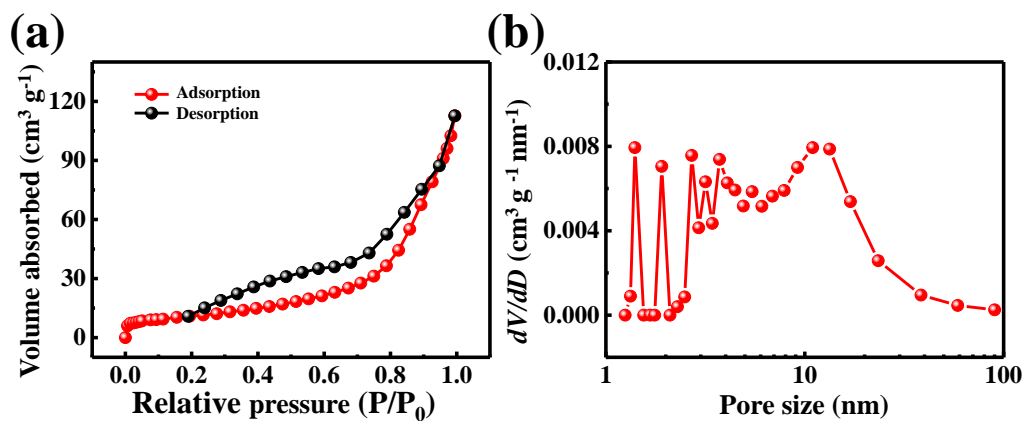
Figure S8. O 1s spectrum of Mn_3O_4/rGO.

(a)

(b)

Figure S9. (a) Nitrogen adsorption–desorption isotherms, and b) the corresponding BJH pore size distribution curve of the as-prepared Mn$_3$O$_4$-rGO-2 sample.
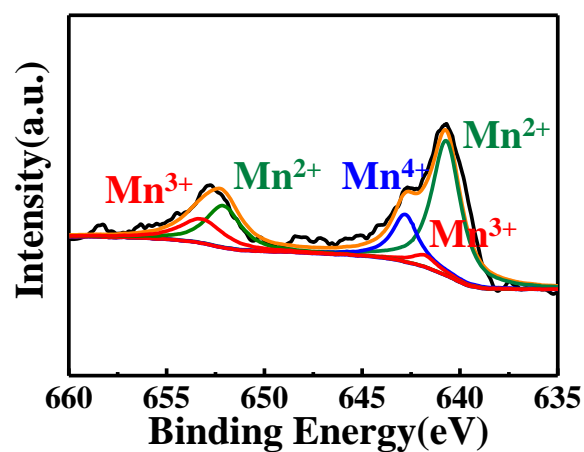

Figure S10. XPS spectrum of Mn 2p of the electrode charged at 0.5 V.
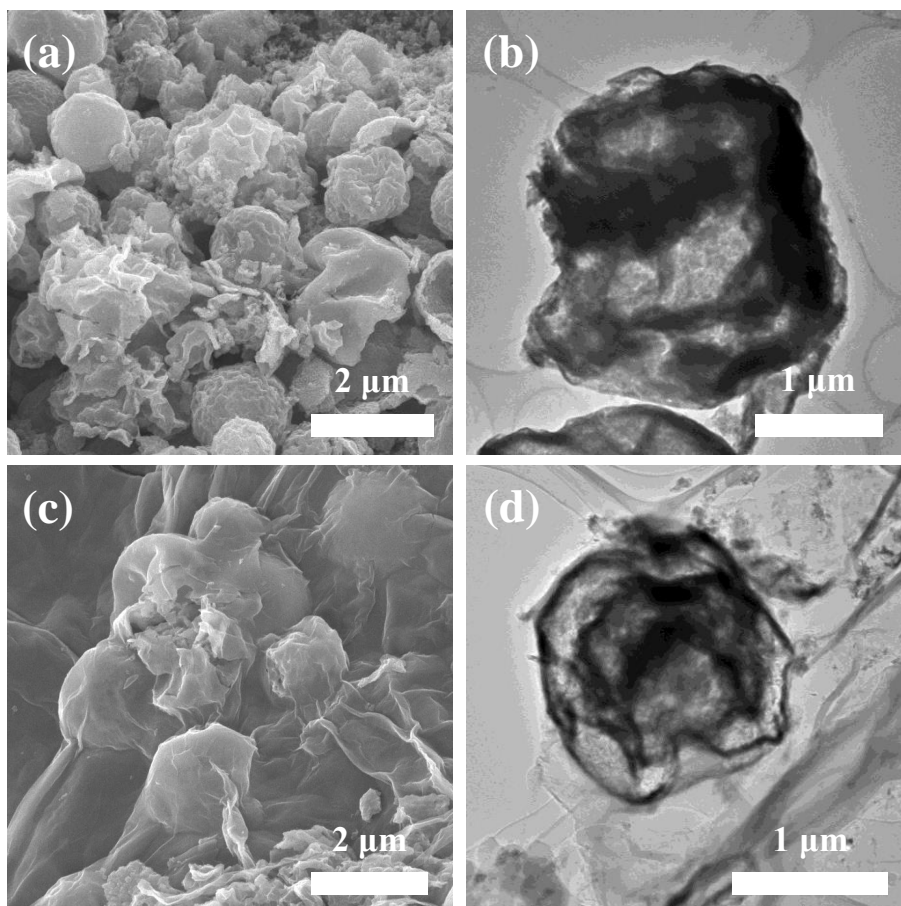
Figure S11. a) SEM and b) TEM image of multi-shelled Mn_3O_4 after 10000 cycles. c) SEM and d) TEM image of Mn_3O_4-rGO-2 after 10000 cycles.
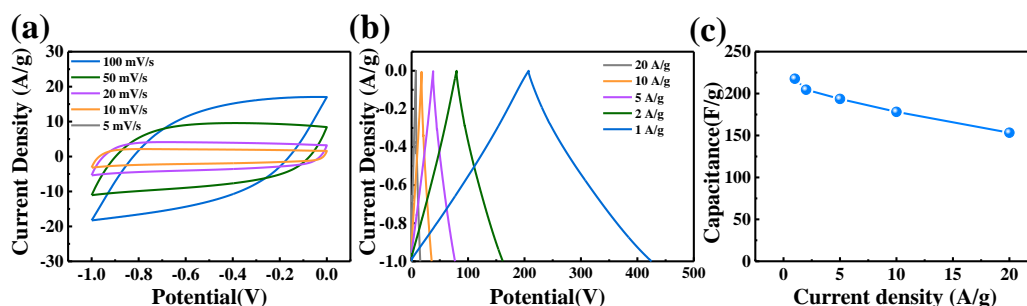
Figure S12. a) CV curves at different scan rates, b) Galvanostatic charge/discharge curves at different current densities, and c) specific capacitances of active carbon electrode.

The electrochemical properties of the active carbon negative electrodes samples were measured using a three-electrode system using KOH aqueous as electrolyte. CV curves of active carbon electrodes were measured in a potential window of -1-0 V at a scan rate from 5 to 100 mV s^{-1}, as shown in Figure S12a. At all scan rates, the CV curves exhibit almost rectangular shape, indicating a typical electrical double layer capacitance behavior. The galvanostatic charge/discharge curves (Figure S12b) display a symmetric triangular shape, demonstrating the high reversibility and ideal capacity of the electric double layer. Figure S12c illustrates the mass specific capacitances of a single electrode versus discharge current density, from 1 to 20 A g^{-1}. At a current density of 1 A g^{-1}, active carbon electrode exhibits the specific capacitance of 217.7 F g^{-1}, and at the high current density of 20 A g^{-1}, the active carbon electrode shows the capacitance of 153 F g^{-1}.
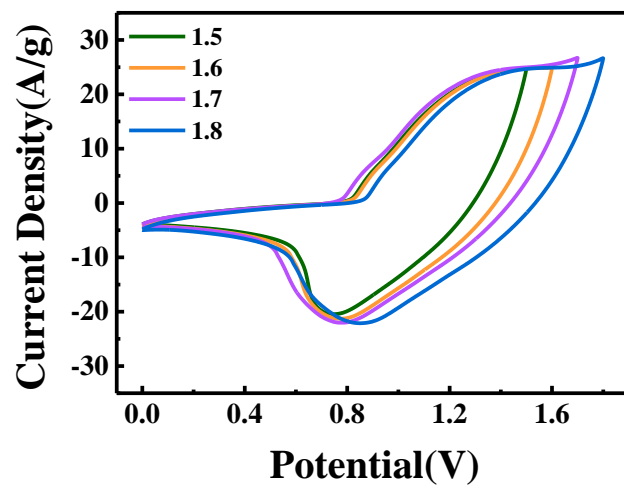
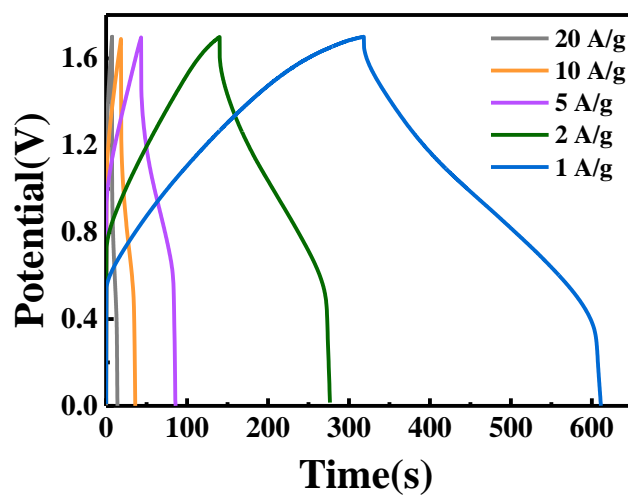**Figure S13.** CV curves of $Mn_3O_4/rGO-2//AC$ at different voltage windows.

Figure S14. GCD curves of the ASC device measured at different current densities.

Table S1. The Mn-O-C and Mn-O-Mn contents in all Mn_3O_4-rGO samples.

	Samples		
	Mn_3O_4-rGO-1	Mn_3O_4-rGO-2	Mn_3O_4-rGO-3
Mn-O-Mn	62.9%	57.9%	59.1%
Mn-O-C	37.1%	42.1%	40.9%